R. & M. No. 3392

MINISTRY OF AVIATION

AERONAUTICAL RESEARCH COUNCIL
REPORTS AND MEMORANDA

On the Axial Compression of Long, Slightly Curved Panels

By G. G. Pope, Ph.D.

LONDON: HER MAJESTY'S STATIONERY OFFICE
1965
PRICE 12s. 0d. NET

On the Axial Compression of Long, Slightly Curved Panels

By G. G. Pope, Ph.D.

Communicated by the Deputy Controller Aircraft (Research and Development), Ministry of Aviation

*Reports and Memoranda No. 3392**

October, 1963

Summary.

A finite-deflection analysis is given of the buckling of long, slightly curved panels in compression parallel to the generators, with sides either clamped or simply-supported, and with various combinations of boundary conditions in the middle surface.

LIST OF CONTENTS

Section

1. Introduction
2. Basic Analysis
3. Application to Specific Panels
   - 3.1 Clamped sides
   - 3.2. Simply-supported sides
4. Middle-Surface Boundary Conditions
   - 4.1 Panel unrestrained in the middle surface
   - 4.2 Boundary conditions along stiff edge members
5. Discussion of Results
   - 5.1 Theoretical results
   - 5.2 Comparison with experimental results

Notation

References

Appendix—Coefficients used in equations (11), (12), (15) and (16) for a_0 and a_1

Illustrations—Figs. 1 to 15

Detachable Abstract Cards

* Replaces R.A.E. Report No. Structures 291—A.R.C. 25 600.

LIST OF ILLUSTRATIONS

Figure

1. General form of load/(end strain) curves
2. Notation
3. Load/(end strain) curves for clamped panels with sides unrestrained in the middle surface
4. Load/(end strain) curves for clamped panels with sides held straight but free to move circumferentially
5. Load/(end strain) curves for clamped panels with sides held straight and prevented from moving circumferentially
6. Load/(end strain) curves for simply-supported panels with sides unrestrained in the middle surface
7. Load/(end strain) curves for simply-supported panels with sides held straight but free to move circumferentially
8. Load/(end strain) curves for simply-supported panels with sides held straight and prevented from moving circumferentially
9. Waveform parameters. Clamped panels with sides unrestrained in the middle surface
10. Waveform parameters. Clamped panels with sides held straight but free to move circumferentially
11. Waveform parameters. Clamped panels with sides held straight and prevented from moving circumferentially
12. Waveform parameters. Simply-supported panels with sides unrestrained in the middle surface
13. Waveform parameters. Simply-supported panels with sides held straight but free to move circumferentially
14. Waveform parameters. Simply-supported panels with sides held straight and prevented from moving circumferentially
15. Comparison of theoretical and experimental load/(end strain) curves

---

1. *Introduction.*

This report presents an approximate analysis of the finite deformation of long, slightly curved panels in uniform compression parallel to the generators, with clamped or simply-supported sides, and with each of the following boundary conditions in the middle surface:

(a) sides unrestrained,

(b) sides held straight in uniform longitudinal strain, but free to move circumferentially,

(c) sides held straight in uniform longitudinal strain and completely restrained against circumferential movement.

The range of curvature over which the analysis is valid depends on the boundary conditions and is discussed in Section 5.2, where the results are compared with those of experimental investigations by Cox and Clenshaw[1] and by Jackson and Hall[2].

In general the theoretical relationship between the mean end load and the mean end strain in a long perfect panel can be expressed as two curves, as shown in Fig. 1a. When the sides are free to move circumferentially, the unbuckled deformation consists of pure compression and OA in Fig. 1a is a straight line. The intersection A with the post-buckled curve then represents the small-deflection-theory buckling load at which the amplitude of the deflection in the post-buckled configuration is also zero; the theoretical curves thus give a complete description of the transition from the unbuckled to the buckled state provided that, in addition, the curvature of the panel is sufficiently small for the mean end load to increase monotonically, and hence in a stable manner, with the mean end strain. For increasing values of the panel curvature the post-buckled curve becomes progressively less stable, as shown in Fig. 1b, and the onset of buckling then depends to a greater extent on initial imperfections and on local constraints at the ends. Nevertheless the perfect-panel analysis should give a good estimate of the minimum end load at which buckling is likely to occur. The interpretation of the more complicated theoretical relationship between the end load and the end strain when the sides of the panel are restrained circumferentially is discussed in Section 5.1.

The analysis given here is based on the assumption that the form of the deflection across the width of the panel in the post-buckled state is the same as that at the small-deflection-theory buckling load. The deflection of the panel centre-line is then assumed to be the sum of a periodic component of arbitrary wavelength and a uniform inward component. This form of the deflection agrees well with Jackson and Hall's experimental results for panels of small curvature; for panels of larger curvature, however, the true deflected shape after buckling tends to resemble the diamond pattern which is characteristic of the buckling in compression of complete cylindrical shells, and this analysis ceases to be applicable. The experimental results also show that the end effects are very local in long panels and are thus unlikely to affect significantly the load/(end strain) curve at a fixed wavelength of deformation. It should, however, be noted that changes in wavelength are impeded by the boundary conditions at the ends. These boundary conditions not only restrict the possible wavelengths of deformation but also tend to stabilise the established buckled form even when the strain energy in other possible buckled forms would be less; the wavelength thus tends to change in sudden jumps. The resulting discontinuities in the load/(end strain) curve, which are neglected in this report, should not influence the results significantly provided that the length/width ratio is greater than, say, 4.

Equations determining the amplitudes of the two components of the assumed form of the deflection at a given wavelength are derived using the principle of virtual displacements; all boundary conditions on the sides are satisfied exactly. The load/(end strain) curve corresponding to the least possible end load at a given end strain is then obtained as the envelope of all such curves when the wavelength is varied. This gives a safer guide to the buckling behaviour than the load/(end strain) curve obtained by minimising the strain energy with respect to the wavelength, because of the restrictions imposed on the possible wavelengths of deformation by the end conditions in panels of finite length. Thus even a long panel may conceivably buckle into a configuration in which the wavelength is such that the end load at a specific mean end strain is less than that at the wavelength appropriate to an infinitely long panel. When the sides of the panel are free to move circumferentially and the panel curvature is small enough for the end load to increase monotonically with the end strain, the difference between these curves is negligible; when the panel curvature is larger, however,

these curves may differ appreciably in the immediate vicinity of the end strain at which the end load is a minimum. Panels with sides prevented from moving circumferentially behave similarly over a much more limited range of curvature, as described in Section 5.1.

The results obtained here are in agreement with Koiter's[3] conjecture that, when the sides of slightly curved panels are free to move circumferentially, the post-buckled load/(end strain) curves converge as the strain is increased with that of the equivalent flat plate. Furthermore, comparing the results of this analysis with those obtained for the flat plate by Koiter[4] and by Stein[5], who use more general expressions for the deflection, it can be shown that this convergence is virtually complete at end strains small enough for the deflected shape assumed here to be sufficiently accurate. The combination of the present analysis and suitable more detailed flat-plate analyses thus specifies satisfactorily over the complete practical range the load/(end strain) curve for slightly curved panels with sides free to move circumferentially.

The bibliography of the buckling theory of curved panels is small compared to that of the related flat-plate and cylindrical-shell problems. The small-deflection-theory buckling loads for clamped and simply-supported curved panels with the middle-surface boundary conditions specified by (b) above have been calculated exactly by Leggett[6], and approximate energy solutions have also been given by Timoshenko and Gere[7] and by Redshaw[8, 9]. An analysis by Koiter[3] of the slope of the load/(end strain) curve in the immediate vicinity of the small-deflection-theory buckling load, for somewhat different boundary conditions to those considered here, is the only rigorous finite deformation solution so far available. Previous approximate energy analyses by Cox and Pribram[10] and by Volmir[11] make considerable simplifying assumptions which, with the advent of the electronic digital computer, are now no longer necessary; both papers, however, give useful indications of the effect of initial imperfections. No analysis has yet been published of the influence of local end constraints on the buckling load of panels; the influence of these constraints in the corresponding problem in the buckling of cylindrical shells has, however, been illustrated by the recent papers by Nachbar and Hoff[12] and by Fischer[13].

2. *Basic Analysis.*

A history and derivation of the basic equations used in this section is given by Mushtari and Galimov[14]. These equations are applicable to shallow cylindrical shells when the maximum deflection is small compared to all the dimensions other than the thickness. Here the range of validity of the analysis is further restricted by the assumed form of the deflection.

The x and s axes lie in the middle surface of a long curved panel of radius R and thickness t, as shown in Fig. 2. The x axis is parallel to the generators and the sides are defined by $s = \pm b$. The analysis may be conveniently expressed in terms of the following non-dimensional notation:

$$S = \frac{s}{b}, \qquad X = \frac{x}{b},$$

$$W = \frac{2\sqrt{3}}{\pi}(1-\nu^2)^{1/2}\frac{w}{t}, \quad k = \frac{(2b)^2}{Rt}(1-\nu^2)^{1/2}$$

where w is the radial deflection.

Similarly the middle-surface stresses σ_x, σ_s and σ_{xs} may be expressed in terms of a non-dimensional stress function ϕ such that

$$\sigma_x = E\epsilon_0 \frac{\partial^2\phi}{\partial S^2}, \qquad \sigma_s = E\epsilon_0 \frac{\partial^2\phi}{\partial X^2}, \qquad \sigma_{xs} = -E\epsilon_0 \frac{\partial^2\phi}{\partial X \partial S} \tag{1}$$

where ϵ_0 is defined, for convenience, as the end strain at buckling in a long flat strip in uniform compression with simply-supported sides unrestrained in its own plane:

$$\epsilon_0 = -\frac{\pi^2}{12(1-\nu^2)}\left(\frac{t}{b}\right)^2. \tag{2}$$

The stress function ϕ then satisfies the equation

$$\nabla^4\phi = -\left(\frac{\partial^2 W}{\partial X \partial S}\right)^2 + \frac{\partial^2 W}{\partial X^2}\left(\frac{\partial^2 W}{\partial S^2} - \frac{\sqrt{3}}{2\pi}k\right), \tag{3}$$

and the displacements u and v in the x and s directions respectively are related to the stresses and to the radial deflection by

$$\frac{1}{\epsilon_0}\frac{\partial u}{\partial x} = \frac{\partial^2\phi}{\partial S^2} - \nu\frac{\partial^2\phi}{\partial X^2} + \frac{1}{2}\left(\frac{\partial W}{\partial X}\right)^2, \tag{4}$$

$$\frac{1}{\epsilon_0}\frac{\partial v}{\partial s} = \frac{\partial^2\phi}{\partial X^2} - \nu\frac{\partial^2\phi}{\partial S^2} + \frac{\sqrt{3}}{2\pi}kW + \frac{1}{2}\left(\frac{\partial W}{\partial S}\right)^2, \tag{5}$$

$$\frac{1}{\epsilon_0}\left(\frac{\partial u}{\partial s} + \frac{\partial v}{\partial x}\right) = -2(1+\nu)\frac{\partial^2\phi}{\partial X \partial S} + \frac{\partial W}{\partial X}\frac{\partial W}{\partial S}. \tag{6}$$

The deflection of the panel is assumed to be of the form

$$W = (a_0 \sin \lambda X + a_1)\Psi(S) \tag{7}$$

where a_0 and a_1 are unspecified coefficients and where the function $\Psi(S)$ represents approximately the form of the deflection across the panel at the small-deflection-theory buckling load. Note that in the unbuckled state it is only necessary for the coefficient a_0 to be zero. The stress function corresponding to this deflected form is found exactly by substituting equation (7) in equation (3) and solving for ϕ. Equations for the constants a_0 and a_1 are then obtained by applying the principle of virtual displacements in conjunction with infinitesimal displacements of the panel given by

$$\delta W_0 = \Psi(S)\delta a_0 \sin \lambda X \tag{8}$$

and

$$\delta W_1 = \Psi(S)\delta a_1. \tag{9}$$

At a fixed value of the wavelength the principle of virtual displacements may be expressed in the form[14]

$$\int_{-1}^{+1}\int_0^{2\pi/\lambda} \delta W \left\{\nabla^4 W + \pi\left[\pi\left(\frac{\partial^2\phi}{\partial X^2}\frac{\partial^2 W}{\partial S^2} - 2\frac{\partial^2\phi}{\partial X \partial S}\frac{\partial^2 W}{\partial X \partial S} + \frac{\partial^2\phi}{\partial S^2}\frac{\partial^2 W}{\partial X^2}\right) - \right.\right.$$
$$\left.\left. - \frac{\sqrt{3}}{2}k\frac{\partial^2\phi}{\partial X^2}\right]\right\} dX\,dS = 0 \tag{10}$$

where δW is an infinitesimal arbitrary variation satisfying all the boundary conditions. For reasons given in the Introduction infinitesimal variations of the wavelength are not considered.

Substituting now equation (7) and the corresponding stress function ϕ into equation (10), and considering in turn the infinitesimal variations of the deflection given by equations (8) and (9), equations of the following form are obtained for the unknown coefficients a_0 and a_1:

$$a_0\{(I_1+I_2+I_3)a_0^2 + I_4a_1^2 + k(L_1-L_2)a_1 - J_1 + \eta_1 J_2 - \eta_2 M_1 - k^2 J_3\} = 0, \tag{11}$$

$$(I_4+I_5+I_6)a_0^2a_1 + k(L_1+L_3+L_4)a_0^2 - (J_4+2\eta_2 M_1)a_1 + k\eta_2 M_2 = 0, \tag{12}$$

where

$$\eta_1 = \frac{\sigma_1}{E\epsilon_0}, \quad \eta_2 = \frac{\sigma_2}{E\epsilon_0}$$

and σ_1 and σ_2 are the mean end and hoop stresses respectively. All the unspecified constants in these and in subsequent equations in this section depend on the boundary conditions and are defined in the subsequent sections.

If the edges of the panel are free to move circumferentially then

$$\eta_2 = 0 \tag{13}$$

and equations (11) and (12) may be combined to form a cubic equation for either a_0^2 or a_1. Under these conditions the coefficient a_1 is also zero if the panel is not buckled.

If the sides are completely restrained in the circumferential direction, the panel experiences a hoop compression which is evaluated by substituting the assumed deflected form into equation (5) and integrating across the panel, giving

$$\eta_2 = \nu\eta_1 - kH_1a_1 - H_2(a_0^2+2a_1^2). \tag{14}$$

The following equations for the coefficients a_0 and a_1 are then obtained by substituting equation (14) in equations (11) and (12).

$$a_0\{(I_1+I_2+I_3+H_2M_1)a_0^2 + (I_4+2H_2M_1)a_1^2 + k(L_1-L_2+H_1M_1)a_1 - J_1 + \eta_1(J_2-\nu M_1) - k^2J_3\} = 0, \tag{15}$$

and

$$(I_4+I_5+I_6+2H_2M_1)a_0^2a_1 + k(L_1+L_3+L_4-H_2M_2)a_0^2 + 4H_2M_1a_1^3 + 2k(H_1M_1-H_2M_2)a_1^2 - (J_4+2\nu\eta_1M_1+k^2H_1M_2)a_1 + \nu\eta_1kM_2 = 0. \tag{16}$$

These may be combined to form a cubic equation for a_1. It will be noted that in the unbuckled state, with these boundary conditions, the panel deflects radially and a_1 is not zero.

3. *Application to Specific Panels.*

In this section the functions used to describe the form of the deflection across clamped and simply-supported panels are specified, together with the constants in equations (11), (12), (15) and (16) derived from them.

3.1. *Clamped Sides.*

The form of the deflection across a panel with clamped sides is here represented by

$$\Psi(S) = \cosh pS - q\cos pS \tag{17}$$

where p is the first positive root (2·36502) of the equation

$$\left.\begin{aligned} \sinh p\cos p + \cosh p\sin p &= 0 \\ \text{and} \qquad q &= \frac{\cosh p}{\cos p}. \end{aligned}\right\} \tag{18}$$

The small-deflection-theory buckling load calculated using this assumed form of the deflection for panels with the middle-surface boundary conditions specified by (b) in Section 1, is within 4% of the exact value calculated by Leggett[6] over the range of curvature considered; in the limiting case of a flat plate the error is less than 1%. The middle-surface stress function corresponding to this deflected form, which satisfies the condition that the mean end strain over a complete cycle of the deflection function along the panel is independent of S, is given by

$$\begin{aligned}\phi = {} & \frac{1}{2}(\eta_1 S^2 + \eta_2 X^2) - \frac{a_0^2\lambda^2}{32p^2}(\cosh 2pS - q^2\cos 2pS - 8q\sinh pS\sin pS) + \\ & + \left\{\frac{\sqrt{3}ka_0\lambda^2}{2\pi}(g_0\cosh pS + g_1\cos pS + b_0\cosh\lambda S + b_1 S\sinh\lambda S) - \right. \\ & \left. - \frac{a_0a_1\lambda^2p^2}{2}(g_2\cosh 2pS + g_3\cos 2pS + 16g_6 + b_2\cosh\lambda S + b_3 S\sinh\lambda S)\right\}\sin\lambda X - \\ & - \frac{a_0^2\lambda^2p^2}{2}(g_4\sinh pS\sin pS + g_5\cosh pS\cos pS - g_6 + b_4\cosh 2\lambda S + b_5 S\sinh 2\lambda S)\cos 2\lambda X \end{aligned} \tag{19}$$

where

$$\left.\begin{aligned} g_0 &= \frac{1}{(p^2-\lambda^2)^2}, & g_1 &= \frac{-q}{(p^2+\lambda^2)^2}, & g_2 &= \frac{1}{(4p^2-\lambda^2)^2}, \\ g_3 &= \frac{-q^2}{(4p^2+\lambda^2)^2}, & g_4 &= \frac{q(4\lambda^4-p^4)}{4(4\lambda^4+p^4)^2}, & g_5 &= \frac{q\lambda^2p^2}{(4\lambda^4+p^4)^2}, \\ & & g_6 &= -\frac{q^2-1}{16\lambda^4} \end{aligned}\right\} \tag{20}$$

and the coefficients b_0 to b_5, which depend on the boundary conditions in the middle surface, are given in Section 4.1.

The constants required in the equations for a_0 and a_1 are given by

$$\left.\begin{aligned} H_1 &= \frac{\sqrt{3}}{4\pi}l_{17}, & H_2 &= -\frac{p^2l_2}{8}, \\ I_1 &= p^4\lambda^3\pi^2(g_5l_1 - g_6l_2 + b_4m_0 + b_5m_1), \\ I_2 &= -\frac{\lambda^3\pi^2}{8}[l_3 - 4p^2\{p^2(g_4l_4 - g_5l_5) + 2\lambda(\lambda b_4 + b_5)m_2 + 2\lambda^2b_5m_3\}], \\ I_3 &= p^3\lambda^3\pi^2\{p(g_4+g_5)l_6 + p(g_4-g_5)l_7 + (2\lambda b_4 + b_5)m_4 + 2\lambda b_5m_5\}, \\ I_4 &= -\frac{p^4\lambda^3\pi^2}{2}(g_2l_8 + g_3l_9 + 16g_6l_2 + b_2m_6 + b_3m_7), \\ I_5 &= -\frac{p^2\lambda^3\pi^2}{2}\{4p^2(g_2l_{18} - g_3l_{19}) + \lambda(\lambda b_2 + 2b_3)m_{10} + \lambda^2b_3m_{11}\}, \\ I_6 &= -p^3\lambda^3\pi^2\{2p(g_2l_{20} - g_3l_{21}) + (\lambda b_2 + b_3)m_{12} + \lambda b_3m_{13}\}, \\ J_1 &= \frac{1}{\lambda}\{(\lambda^4+p^4)l_{10} - 2\lambda^2p^2l_2\}, \\ J_2 &= \lambda\pi^2l_{10}, \end{aligned}\right\} \tag{21}$$

contd.

$$
\left.
\begin{aligned}
J_3 &= \frac{3\lambda^3}{4}(g_0 l_{11} + g_1 l_{12} + b_0 m_8 + b_1 m_9), \\
J_4 &= \frac{2p^4}{\lambda} l_{10}, \\
L_1 &= \frac{\sqrt{3}p^2\lambda^3\pi}{2}(g_0 l_{13} + g_1 l_{14} + b_0 m_6 + b_1 m_7), \\
L_2 &= -\frac{\sqrt{3}p^2\lambda^3\pi}{4}(g_2 l_{15} + g_3 l_{16} + 16 g_6 l_{17} + b_2 m_8 + b_3 m_9), \\
L_3 &= \frac{\sqrt{3}\lambda^3\pi}{2}\{-2p^2(g_0 l_{22} - g_1 l_{23}) + \lambda(\lambda b_0 + 2b_1)m_{10} + \lambda^2 b_1 m_{11}\}, \\
L_4 &= \sqrt{3}p\lambda^3\pi\{p(g_0 l_{22} - g_1 l_{23}) + (\lambda b_0 + b_1)m_{12} + \lambda b_1 m_{13}\}, \\
M_1 &= \frac{p^2\pi^2 l_2}{\lambda}, \qquad M_2 = \frac{\sqrt{3}\pi l_{17}}{\lambda}.
\end{aligned}
\right\} \qquad (21)\ \textit{contd.}
$$

The integrals l_i, which are constants, and m_i, which are functions of λ, are listed in the Appendix.

The mean end strain in the panel in this deflected form is given by $\epsilon\epsilon_0$ where

$$\epsilon = \eta_1 - \nu\eta_2 + \frac{a_0^2\lambda^2}{8}(q^2+1). \qquad (22)$$

3.2. *Simply-Supported Sides.*

The form of the deflection across a panel with simply-supported sides is here represented by

$$\Psi(S) = \cos\frac{\pi S}{2}. \qquad (23)$$

The small-deflection-theory buckling load calculated using this assumed form of the deflection for panels with the middle-surface boundary conditions specified by (b) in Section 1 is within 1% of the exact value calculated by Leggett[6] over the range of curvature considered; the exact value is obtained in the limiting case of a flat plate. Thus the slope of the post-buckled curve at the instant of buckling is also obtained exactly for the flat plate (*see* Mansfield[15]). The middle-surface stress function corresponding to the assumed deflected form, which satisfies the condition that the mean end strain over a complete cycle of the deflection function along the panel is independent of S, is given by

$$
\begin{aligned}
\phi = \frac{1}{2}(\eta_1 S^2 + \eta_2 X^2) + \frac{a_0^2\lambda^2}{8\pi^2}\cos\pi S + \Big\{ & \frac{\sqrt{3}ka_0\lambda^2}{2\pi}\left(h_0\cos\frac{\pi S}{2} + b_0\cosh\lambda S + b_1 S\sinh\lambda S\right) - \\
& - \frac{a_0 a_1\lambda^2\pi^2}{8}(h_1\cos\pi S + 16h_2 + b_2\cosh\lambda S + b_3 S\sinh\lambda S)\Big\}\sin\lambda X - \\
& - \frac{a_0^2\lambda^2\pi^2}{8}(-h_2 + b_4\cosh 2\lambda S + b_5 S\sinh 2\lambda S)\cos 2\lambda X
\end{aligned}
\qquad (24)
$$

where

$$h_0 = \frac{16}{(\pi^2+4\lambda^2)^2}, \qquad h_1 = -\frac{1}{(\pi^2+\lambda^2)^2}, \qquad h_2 = -\frac{1}{16\lambda^4} \qquad (25)$$

and the coefficients b_0 to b_5, which depend on the boundary conditions in the middle surface, are given in Section 4.2.

The constants required in the equations for a_0 and a_1 are given by

$$
\left.
\begin{aligned}
H_1 &= \frac{\sqrt{3}}{\pi^2}, \qquad H_2 = \frac{\pi^2}{32},\\
I_1 &= \frac{\lambda^3\pi^6}{16}(h_2 + b_4 n_0 + b_5 n_1),\\
I_2 &= -\frac{\lambda^3\pi^2}{16}[1 + 4\lambda\pi^2\{(\lambda b_4 + b_5)n_0 + \lambda b_5 n_1\}],\\
I_3 &= \frac{\lambda^3\pi^5}{8}\{(2\lambda b_4 + b_5)n_2 + 2\lambda b_5 n_3\},\\
I_4 &= \frac{\lambda^3\pi^6}{64}(h_1 + 32h_2 - 2b_2 n_4 - 2b_3 n_5),\\
I_5 &= \frac{\lambda^3\pi^4}{16}\{\pi^2 h_1 + 2\lambda(\lambda b_2 + 2b_3)n_4 + 2\lambda^2 b_3 n_5\},\\
I_6 &= -\frac{\lambda^3\pi^5}{16}\{\pi h_1 + 2(\lambda b_2 + b_3)n_8 + \lambda b_3 n_9\},\\
J_1 &= \frac{1}{16\lambda}(4\lambda^2 + \pi^2)^2,\\
J_2 &= \lambda\pi^2,\\
J_3 &= \frac{3\lambda^3}{4}(h_0 + b_0 n_6 + b_1 n_7),\\
J_4 &= \frac{\pi^4}{8\lambda},\\
L_1 &= \frac{\sqrt{3}\lambda^3\pi^3}{8}\left\{-\frac{8h_0}{3\pi} + b_0 n_4 + b_1 n_5\right\},\\
L_2 &= -\frac{\sqrt{3}\lambda^3\pi^3}{16}\left\{\frac{4}{3\pi}(h_1 + 48h_2) + b_2 n_6 + b_3 n_7\right\},\\
L_3 &= -\frac{\sqrt{3}\lambda^3\pi}{2}\left\{\frac{2\pi}{3}h_0 + \lambda(\lambda b_0 + 2b_1)n_4 + \lambda^2 b_1 n_5\right\},\\
L_4 &= \frac{\sqrt{3}\lambda^3\pi^2}{2}\left\{\frac{2h_0}{3} + (\lambda b_0 + b_1)n_8 + \lambda b_1 n_9\right\},\\
M_1 &= -\frac{\pi^4}{4\lambda}, \quad , \quad M_2 = \frac{4\sqrt{3}}{\lambda}.
\end{aligned}
\right\} \tag{26}
$$

The integrals n_i are listed in the Appendix.

The mean end strain in the panel in this deflected form is given by $\epsilon\epsilon_0$ where

$$\epsilon = \eta_1 - \nu\eta_2 + \frac{a_0^2\lambda^2}{8}. \tag{27}$$

4. *Middle-Surface Boundary Conditions at Sides.*

In this section the constants b_0 to b_5 are evaluated for the specific combinations of boundary conditions considered in this report. The algebraic form of these constants is the same whether or not the sides are free to move circumferentially.

4.1. *Panel Unrestrained in the Middle Surface.*

Consider first the sides supported in such a way that the panel is unrestrained in the middle surface. The constants b_0 to b_5 are obtained from the boundary conditions

$$\frac{\partial^2\phi}{\partial X^2} = 0 \quad \text{and} \quad \frac{\partial^2\phi}{\partial X \partial S} = 0. \tag{28}$$

This somewhat impractical combination of boundary conditions is included for comparison with previous experimental results.

4.1.1. *Clamped sides.*—The following expressions for the constants b_0 to b_5 are obtained by substituting equation (19) in equations (28):

$$\begin{aligned}
b_0 \cosh\lambda &= -(g_0 \cosh p + g_1 \cos p + b_1 \sinh\lambda), \\
b_1(2\lambda + \sinh 2\lambda) &= 2\{g_0(\lambda \cosh p \sinh\lambda - p \sinh p \cosh\lambda) + \\
&\quad + g_1(\lambda \cos p \sinh\lambda + p \sin p \cosh\lambda)\}, \\
b_2 \cosh\lambda &= -(g_2 \cosh 2p + g_3 \cos 2p + 16 g_6 + b_3 \sinh\lambda), \\
b_3(2\lambda + \sinh 2\lambda) &= 2\{g_2(\lambda \cosh 2p \sinh\lambda - 2p \sinh 2p \cosh\lambda) + \\
&\quad + g_3(\lambda \cos 2p \sinh\lambda + 2p \sin 2p \cosh\lambda) + 16 g_6 \lambda \sinh\lambda\}, \\
b_4 \cosh 2\lambda &= -(g_4 \sinh p \sin p + g_5 \cosh p \cos p - g_6 + b_5 \sinh 2\lambda), \\
b_5(4\lambda + \sinh 4\lambda) &= 2\{2\lambda \sinh 2\lambda(g_4 \sinh p \sin p + g_5 \cosh p \cos p - g_6) - \\
&\quad - g_5 p \cosh 2\lambda(\sinh p \cos p - \cosh p \sin p)\}.
\end{aligned}$$

4.1.2. *Simply-Supported Sides.*—The following expressions for the constants b_0 to b_5 are obtained by substituting equation (24) in equations (28):

$$\begin{aligned}
b_0 &= -b_1 \tanh\lambda, \\
b_1(2\lambda + \sinh 2\lambda) &= \pi h_0 \cosh\lambda, \\
\lambda b_2 \sinh\lambda &= -b_3(\sinh\lambda + \lambda \cosh\lambda) \\
b_3(2\lambda + \sinh 2\lambda) &= -2\lambda(h_1 - 16 h_2)\sinh\lambda, \\
b_4 \cosh 2\lambda &= h_2 - b_5 \sinh 2\lambda, \\
b_5(4\lambda + \sinh 4\lambda) &= -4\lambda h_2 \sinh 2\lambda.
\end{aligned}$$

4.2. *Boundary Conditions along Stiff Edge Members.*

It is assumed here that the panel is bounded by edge members of sufficiently high rigidity for the normal displacement and the longitudinal strain of the sides to be independent of X. The components

of the end load which are periodic in X under these boundary conditions are, in fact, less than 3% of the mean end load over the range computed.

4.2.1. *Clamped sides.*—Substituting the assumed deflected form, equation (17), and the middle-surface stress function, equation (19), into equations (4) and (5), and integrating the latter across the panel, the following expressions are obtained for the constants b_0 to b_5 by equating the relevant terms to zero.

$$\begin{aligned}
b_0(1+\nu)\lambda^2\cosh\lambda &= -[g_0(p^2+\nu\lambda^2)\cosh p - g_1(p^2-\nu\lambda^2)\cos p + \\
&\quad + \lambda b_1\{2\cosh\lambda + \lambda(1+\nu)\sinh\lambda\}],
\end{aligned}$$

$$\begin{aligned}
&b_1\lambda^2 p\{2\lambda(1+\nu) - (3-\nu)\sinh 2\lambda\} \\
&\quad = \cosh\lambda[pl_{17} - 2\lambda^2\{g_0(\lambda^2+\nu p^2)\sinh p + g_1(\lambda^2-\nu p^2)\sin p\}] + \\
&\quad\quad + 2\lambda p\sin\lambda\{g_0(p^2+\nu\lambda^2)\cosh p - g_1(p^2-\nu\lambda^2)\cos p\},
\end{aligned}$$

$$\begin{aligned}
b_2(1+\nu)\lambda^2\cosh\lambda &= -[g_2(4p^2+\nu\lambda^2)\cosh 2p - g_3(4p^2-\nu\lambda^2)\cos 2p + 16\nu\lambda^2 g_6 + \\
&\quad + \lambda b_3\{2\cosh\lambda + \lambda(1+\nu)\sinh\lambda\}],
\end{aligned}$$

$$\begin{aligned}
&b_3\lambda^2 p\{2\lambda(1+\nu) - (3-\nu)\sinh 2\lambda\} \\
&\quad = \cosh\lambda[2pl_2 - \lambda^2\{g_2(\lambda^2+4\nu p^2)\sinh 2p + g_3(\lambda^2-4\nu p^2)\sin 2p + 32p\lambda^2 g_6\}] + \\
&\quad\quad + 2p\lambda\sinh\lambda\{g_2(4p^2+\nu\lambda^2)\cosh 2p - g_3(4p^2-\nu\lambda^2)\cos 2p + 16\nu\lambda^2 g_6\},
\end{aligned}$$

$$\begin{aligned}
2b_4(1+\nu)\lambda^2\cosh 2\lambda &= -[(p^2 g_4 + 2\nu\lambda^2 g_5)\cosh p\cos p - \\
&\quad - (p^2 g_5 - 2\nu\lambda^2 g_4)\sinh p\sin p - \\
&\quad - 2\nu\lambda^2 g_6 + 2\lambda b_5\{\cosh 2\lambda + \lambda(1+\nu)\sinh 2\lambda\}],
\end{aligned}$$

$$\begin{aligned}
&2b_5\lambda^2 p\{4\lambda(1+\nu) - (3-\nu)\sinh 4\lambda\} \\
&\quad = \cosh 2\lambda[-pl_2 - 4\lambda^2(2\lambda^2 g_5 + \nu p^2 g_4)(\cosh p\sin p - \sinh p\cos p) + 16p\lambda^4 g_6] + \\
&\quad\quad + 4\lambda p\sinh 2\lambda\{(p^2 g_4 + 2\nu\lambda^2 g_5)\cosh p\cos p - (p^2 g_5 - 2\nu\lambda^2 g_4)\sinh p\sin p - 2\nu\lambda^2 g_6\}.
\end{aligned}$$

4.2.2. *Simply-supported sides.*—Substituting the assumed deflected form, equation (23), and the middle-surface stress function, equation (24), into equations (4) and (5), and integrating the latter across the panel, the following expressions are obtained for the constants b_0 to b_5 by equating the relevant terms to zero.

$$\begin{aligned}
b_0(1+\nu)\lambda\cosh\lambda &= -b_1\{2\cosh\lambda + \lambda(1+\nu)\sinh\lambda\}, \\
b_1\lambda^2\pi\{2\lambda(1+\nu) - (3-\nu)\sinh 2\lambda\} &= \cosh\lambda\{4 - \lambda^2 h_0(4\lambda^2 - \nu\pi^2)\}, \\
b_2(1+\nu)\lambda^2\cosh\lambda &= h_1(\pi^2 - \nu\lambda^2) - 16\nu\lambda^2 h_2 - \lambda b_3\{2\cosh\lambda + \lambda(1+\nu)\sinh\lambda\}, \\
b_3\lambda\{2\lambda(1+\nu) - (3-\nu)\sinh 2\lambda\} &= 2\sinh\lambda\{-h_1(\pi^2 - \nu\lambda^2) + 16\nu\lambda^2 h_2\}, \\
b_4(1+\nu)\lambda\cosh 2\lambda &= \nu\lambda h_2 - b_5\{\cosh 2\lambda + \lambda(1+\nu)\sinh 2\lambda\}, \\
b_5\{4\lambda(1+\nu) - (3-\nu)\sinh 4\lambda\} &= -4\nu\lambda h_2\sinh 2\lambda.
\end{aligned}$$

5. *Discussion of Results.*

5.1. *Theoretical Results.*

Graphs showing the variation of the mean-end-load parameter η_1 and the waveform coefficients λ, a_0 and a_1 with the mean-end-strain parameter ϵ and the curvature parameter k are given for long panels with each of the following combinations of boundary conditions:

η_1 Fig.	λ, a_0, a_1 Fig.	
3	9	Clamped sides unrestrained in the middle surface.
4	10	Clamped sides held straight but free to move circumferentially.
5	11	Clamped sides held straight and prevented from moving circumferentially.
6	12	Simply-supported sides unrestrained in the middle surface.
7	13	Simply-supported sides held straight but free to move circumferentially.
8	14	Simply-supported sides held straight and prevented from moving circumferentially.

The characteristic behaviour of curved panels in axial compression with sides free to move circumferentially is comparatively straightforward and is described in the Introduction. The following discussion is concerned, therefore, with the effect of restraining the circumferential movement of the sides.

When a flat panel is compressed axially with transverse displacement of the sides prevented in its own plane, the unbuckled deformation is stiffer than that of a corresponding panel with free transverse deformation by the factor $1/(1-\nu^2)$. When, however, the panel is initially curved across its width and is restrained circumferentially, the curvature increases with end load to relieve the hoop stresses, as shown in Figs. 11 and 14, and thus the unbuckled axial stiffness is less than that of the corresponding flat plate; consequently the stiffness in the unbuckled state varies slightly with the curvature parameter k and with the magnitude of the applied load. The stiffness is, however, virtually identical with that of a panel with free circumferential movement of the sides when k is large. This is illustrated by the results for clamped panels shown in Fig. 5; when, however, the sides are simply supported (Fig. 8), the unbuckled load/(end strain) relationship is indistinguishable from that for panels with free circumferential movement of the sides even at the smallest value of the curvature parameter shown.

For reasons given in the Introduction, the envelope of the post-buckled curves for all possible longitudinal wavelengths of deformation is used in this report to represent the post-buckled behaviour of curved panels. Now, when the sides are free to move circumferentially, the unbuckled and post-buckled load/(end strain) curves always intersect at a bifurcation point (i.e. the amplitudes of the radial-deflection components in the buckled form are both zero, so that the buckled and unbuckled forms coincide). When, however, the sides are prevented from moving circumferentially, the unbuckled and post-buckled curves only intersect at a bifurcation point over a limited range of the wavelength, due to the increase in curvature with end load in the unbuckled state. When the wavelength and the initial curvature are such that the post-buckled curve does not intersect the unbuckled curve at a bifurcation point, the computations show that these have, nevertheless, a

non-bifurcational intersection. The envelope of post-buckled curves only consists entirely of 'bifurcational' curves when the curvature parameter k is less than about 8 for clamped panels or about 1 for simply-supported panels. It is found, however, that the post-buckled curves contributing to the envelope when the end strain is large are 'bifurcational' over the whole of the range of the parameter k for which results are given.

Before assessing the significance of those post-buckled curves which do not intersect the unbuckled curve at bifurcation points, it is useful to consider a curved panel with sides held straight but free to move circumferentially, under steadily increasing axial strain. The sides move apart at first due to the effect of Poisson's ratio, and this movement is increased immediately after buckling by the overall flattening of the panel in the buckled configuration (i.e. the mean deflection of the panel centre-line approaches the plane containing the sides as shown in Figs. 9 to 14). At the same time, however, the periodic radial deflection along the buckled panel causes a second-order reduction in the width, which predominates when the end strain is sufficiently large. Thus, at a specific large value of the end strain, there is again no circumferential displacement of the sides, and the work done on the panel and the configuration of the panel are the same as for a panel with sides prevented from moving circumferentially. Although this end strain is far beyond the range of validity of the present analysis, the value obtained here can, nevertheless, be used to verify the significance of numerical results when the end strain is smaller.

Consider, now, a curved panel constrained to deform in such a way that the deflection of the centre-line has a fixed wavelength, and let this wavelength be so chosen that the post-buckled load/(end strain) curve does not join the unbuckled curve at a bifurcation point if the sides cannot move circumferentially. Computations using this analysis confirm that the appropriate results for such panels with and without circumferential movement of the sides coincide at the relevant large value of the end strain. It is thus indicated that those curves in the envelopes of post-buckled load/(end strain) curves which do not intersect the unbuckled results at bifurcation points have, nevertheless, some practical significance. It must be remembered, however, that everywhere except at this particular large end strain, the presence of circumferential restraint necessarily increases the work done in applying a given end strain to the panel. Now, by comparing Figs. 7 and 8 it is seen that the minimum end load at a given end strain for simply-supported panels appears to be consistently reduced by the presence of circumferential restraint on the sides. Thus the jump to the post-buckled configuration when the sides cannot move circumferentially must necessarily be delayed to a far greater end strain than that at the intersection with the unbuckled curve. Post-buckled curves are therefore only shown in Fig. 8 at relatively large values of the end strain. This is the only combination of boundary conditions considered for which the present type of perfect-panel analysis fails to give a sensible estimate of the minimum end load at which buckling is likely to occur.

5.2. *Comparison with Experimental Results.*

Deductions made in this section regarding the range of curvature over which the theoretical analysis is valid refer only to panels with sides free to move circumferentially; no experimental evidence is available on the reduction in the range of validity when circumferential movement is prevented.

An examination of the available experimental results[1, 2], which were all obtained using panels with clamped sides free to deform in the middle surface, suggests that the assumed deflected shape is adequate under clamped boundary conditions provided the curvature parameter k does not exceed

about 25. On this basis it can be inferred that the theoretical analysis for simply-supported panels can be used when the curvature parameter k is less than about 15. Thus, for example, the analysis is applicable to panels 10 in. wide and 0·128 in. thick provided that the radii of curvature are not less than 30 in. and 50 in. respectively for clamped and simply-supported sides.

Two specimen experimental load/(end strain) curves from Jackson and Hall's paper[2] are compared in Fig. 15 with corresponding theoretical results for an infinitely long panel. The theoretical analysis slightly underestimates the stiffness of the panel immediately after buckling, probably because it takes no account of the restriction imposed by the ends on the possible wavelengths of deformation. The deterioration in accuracy when the end strain is large is due to modifications in the deflected shape which are not allowed for in this analysis. At such values of the end strain however the behaviour of the panel is virtually the same as that of a flat plate, for which more elaborate theoretical results are available[4, 5].

NOTATION

x, s		Cartesian axes along and across the panel
$2b$		Width of panel
R		Radius of curvature of panel
t		Thickness of panel
σ_1, σ_2		Mean end stress and mean hoop stress respectively
w		Radial deflection
u, v		Displacements parallel to the x and s axes respectively
X, S	$=$	$\frac{x}{b}, \frac{s}{b}$
W	$=$	$\frac{2\sqrt{3}}{\pi}(1-\nu^2)^{1/2}\frac{w}{t}$
k	$=$	$\frac{(2b)^2}{Rt}(1-\nu^2)^{1/2}$
ϵ_0	$=$	$-\frac{\pi^2}{12(1-\nu^2)}\left(\frac{t}{b}\right)^2$
ϵ		Mean end strain/ϵ_0
η_1, η_2	$=$	$\frac{\sigma_1}{E\epsilon_0}, \frac{\sigma_2}{E\epsilon_0}$
$\sigma_x, \sigma_s, \sigma_{xs}$		Middle-surface stresses
ϕ		Middle-surface stress function defined by equation (1)
a_0, a_1, λ		Deflection parameters defined by equation (7)
$\Psi(S)$		Assumed form of the deflection across the panel
I_i, L_i, J_i		Constants in equations (11), (12), (15) and (16)
H_i, M_i		Constants in equations (14), (15) and (16)
p, q		Constants defined in equation (18)
g_i, h_i		Constants in stress functions defined respectively in equations (20) and (25)
l_i, m_i, n_i		Constants defined in the Appendix
b_i		Constants defined in Section 4
E		Young's modulus
ν		Poisson's ratio (taken as 0·3 in the computations)
∇^4		Biharmonic operator

REFERENCES

No.	*Author(s)*	*Title, etc.*
1	H. L. Cox and W. J. Clenshaw ..	Compression tests on curved plates of thin sheet Duralumin. A.R.C. R. & M. 1894. November, 1941.
2	K. B. Jackson and A. H. Hall ..	Curved plates in compression. N.R.L. Report MM-180, Ottawa, 1945.
3	W. T. Koiter	Buckling and post-buckling behaviour of a cylindrical panel under axial compression. N.L.L. Report S.476, Amsterdam, 1956.
4	W. T. Koiter	The equivalent width at loads far above the buckling load for various boundary conditions along the plate edges (in Dutch). N.L.L. Report S.287, Amsterdam, 1943.
5	M. Stein	Loads and deformations of buckled rectangular plates. N.A.S.A. Tech. Report R.40. 1959.
6	D. M. A. Leggett	The buckling of a long curved panel under axial compression. A.R.C. R. & M. 1899. July, 1942.
7	S. P. Timoshenko and J. M. Gere	*Theory of elastic stability*, 2nd Edition. McGraw-Hill, New York, 1961.
8	S. C. Redshaw	The elastic instability of a thin curved panel subjected to an axial thrust, its axial and circumferential edges being simply supported. A.R.C. R. & M. 1565. May, 1933.
9	S. C. Redshaw	The elastic instability of a curved plate under axial thrusts. *J. R. Ae. Soc.*, Vol. 42, p. 536. 1938.
10	H. L. Cox and E. Pribram ..	Elements of the buckling of curved plates. *J. R. Ae. Soc.*, Vol. 52, p. 551. 1948.
11	A. S. Volmir	*Elastic plates and shells* (in Russian). Moscow, 1956.
12	W. Nachbar and N. J. Hoff ..	The buckling of a free edge of an axially compressed circular cylindrical shell. *Quart. App. Math.*, Vol. 20, No. 3, p. 267. October, 1962.
13	G. Fischer	Über den Einfluss der gelenkigen Lagerung auf die Stabilität dünnwandiger Kreiszylinderschalen unter Axiallast und Innendruck. *Z. Flugwiss*, Vol. 11, Part 3. 1963.
14	K. M. Mushtari and K. Z. Galimov	Non-linear theory of thin elastic shells. Translated by the Israel program for scientific translations for N.A.S.A. 1961.
15	E. H. Mansfield	Some identities on structural flexibility after buckling. *Aero. Quart.*, Vol. 9. August, 1958.

APPENDIX

Coefficients Used in Equations (11), (12), (15) *and* (16) *for* a_0 *and* a_1

1. *Panel with Clamped Edges.*

(a) *Coefficients which are independent of* λ.

Let

$$\alpha = \sqrt{(q^2-1)}, \qquad \beta = \sqrt{(q^2+1)}.$$

$$l_1 = \frac{\alpha\beta^3}{5pq}, \qquad l_{12} = \frac{\alpha\beta}{2pq} - q,$$

$$l_2 = -\alpha\left(\alpha - \frac{\beta}{p}\right), \qquad l_{13} = -\frac{2\sqrt{2\alpha}}{15p}(q^2-7),$$

$$l_3 = \frac{3\alpha^3\beta}{4p} + \frac{1}{2}(1+8q^2+q^4), \qquad l_{14} = \frac{2\sqrt{2\alpha}}{15pq}(7q^2-1),$$

$$l_4 = -\frac{\alpha^3\beta}{4pq} - q, \qquad l_{15} = \frac{2\sqrt{2\alpha}}{15p}(q^2-2),$$

$$l_5 = -\frac{3\alpha\beta^3}{20pq}, \qquad l_{16} = \frac{2\sqrt{2\alpha}}{15pq^2}(2q^2+1),$$

$$l_6 = \frac{\alpha\beta}{20pq}(q^2-4) + \frac{q}{2}, \qquad l_{17} = \frac{2\sqrt{2\alpha}}{p},$$

$$l_7 = \frac{\alpha\beta}{20pq}(4q^2-1) + \frac{q}{2}, \qquad l_{18} = \frac{\alpha\beta}{20p}(2q^2+7) + \frac{1}{2},$$

$$l_8 = \frac{\alpha\beta}{4p} + \frac{1}{2}, \qquad l_{19} = -\frac{\alpha\beta}{20pq^2}(7q^2+2) + \frac{q^2}{2},$$

$$l_9 = \frac{\alpha\beta}{4p} - \frac{q^2}{2}, \qquad l_{20} = -\frac{\alpha\beta}{20p}(2q^2-13) - \frac{1}{2},$$

$$l_{10} = q^2 + 1, \qquad l_{21} = -\frac{\alpha\beta}{20pq^2}(13q^2-2) - \frac{q^2}{2},$$

$$l_{11} = \frac{\alpha\beta}{2p} + 1, \qquad l_{22} = \frac{4\sqrt{2\alpha}}{15p}(q^2+5),$$

$$l_{23} = -\frac{4\sqrt{2\alpha}}{15p}(5q^2+1).$$

(b) *Coefficients which are dependent on* λ.

The form of the coefficients given below is applicable provided $\lambda \neq p$ and $\lambda \neq 2p$.

$$m_0 = \frac{1}{2}\left\{\frac{\sinh 2(\lambda+p)}{2(\lambda+p)} + \frac{\sinh 2(\lambda-p)}{2(\lambda-p)}\right\} -$$

$$- \frac{q^2}{2(\lambda^2+p^2)}(\lambda \sinh 2\lambda \cos 2p + p \cosh 2\lambda \sin 2p) - \alpha^2 \frac{\sinh 2\lambda}{2\lambda},$$

$$m_1 = \frac{1}{2}\left\{\frac{\cosh 2(\lambda+p)}{2(\lambda+p)} + \frac{\cosh 2(\lambda-p)}{2(\lambda-p)} - \frac{\sinh 2(\lambda+p)}{4(\lambda+p)^2} - \frac{\sinh 2(\lambda-p)}{4(\lambda-p)^2}\right\} -$$

$$- \alpha^2\left(\frac{\cosh 2\lambda}{2\lambda} - \frac{\sinh 2\lambda}{4\lambda^2}\right) - \frac{q^2}{2(\lambda^2+p^2)}(\lambda\cosh 2\lambda\cos 2p + p\sinh 2\lambda\sin 2p) +$$

$$+ \frac{q^2}{4(\lambda^2+p^2)^2}\{(\lambda^2-p^2)\sinh 2\lambda\cos 2p + 2\lambda p\cosh 2\lambda\sin 2p\},$$

$$m_2 = \frac{1}{2}\left\{\frac{\sinh 2(\lambda+p)}{2(\lambda+p)} + \frac{\sinh 2(\lambda-p)}{2(\lambda-p)}\right\} +$$

$$+ \frac{q^2}{2(\lambda^2+p^2)}(\lambda\sinh 2\lambda\cos 2p + p\cosh 2\lambda\sin 2p) -$$

$$- \frac{2q}{(2\lambda+p)^2+p^2}\{(2\lambda+p)\sinh(2\lambda+p)\cos p + p\cosh(2\lambda+p)\sin p\} -$$

$$- \frac{2q}{(2\lambda-p)^2+p^2}\{(2\lambda-p)\sinh(2\lambda-p)\cos p + p\cosh(2\lambda-p)\sin p\} + \beta^2\frac{\sinh 2\lambda}{2\lambda},$$

$$m_3 = \frac{1}{2}\left\{\frac{\cosh 2(\lambda+p)}{2(\lambda+p)} + \frac{\cosh 2(\lambda-p)}{2(\lambda-p)} - \frac{\sinh 2(\lambda+p)}{4(\lambda+p)^2} - \frac{\sinh 2(\lambda-p)}{4(\lambda-p)^2}\right\} +$$

$$+ \beta^2\left(\frac{\cosh 2\lambda}{2\lambda} - \frac{\sinh 2\lambda}{4\lambda^2}\right) + \frac{q^2}{2(\lambda^2+p^2)}(\lambda\cosh 2\lambda\cos 2p + p\sinh 2\lambda\sin 2p) -$$

$$- \frac{q^2}{4(\lambda^2+p^2)^2}\{(\lambda^2-p^2)\sinh 2\lambda\cos 2p + 2\lambda p\cosh 2\lambda\sin 2p\} -$$

$$- \frac{2q}{(2\lambda+p)^2+p^2}\{(2\lambda+p)\cosh(2\lambda+p)\cos p + p\sinh(2\lambda+p)\sin p\} +$$

$$+ \frac{2q}{\{(2\lambda+p)^2+p^2\}^2}\{[(2\lambda+p)^2 - p^2]\sinh(2\lambda+p)\cos p + 2(2\lambda+p)p\cosh(2\lambda+p)\sin p\} -$$

$$- \frac{2q}{(2\lambda-p)^2+p^2}\{(2\lambda-p)\cosh(2\lambda-p)\cos p + p\sinh(2\lambda-p)\sin p\} +$$

$$+ \frac{2q}{\{(2\lambda-p)^2+p^2\}^2}\{[(2\lambda-p)^2 - p^2]\sinh(2\lambda-p)\cos p + 2(2\lambda-p)p\cosh(2\lambda-p)\sin p\},$$

$$m_4 = \frac{1}{2}\left\{\frac{\sinh 2(\lambda+p)}{2(\lambda+p)} - \frac{\sinh 2(\lambda-p)}{2(\lambda-p)}\right\} - \frac{q^2}{2(\lambda^2+p^2)}(\lambda\cosh 2\lambda\sin 2p - p\sinh 2\lambda\cos 2p) -$$

$$- \frac{2q}{(2\lambda+p)^2+p^2}\{(\lambda+p)\sinh(2\lambda+p)\cos p - \lambda\cosh(2\lambda+p)\sin p\} +$$

$$+ \frac{2q}{(2\lambda-p)^2+p^2}\{\lambda\cosh(2\lambda-p)\sin p + (\lambda-p)\sinh(2\lambda-p)\cos p\},$$

$$m_5 = \frac{1}{2}\left\{\frac{\cosh 2(\lambda+p)}{2(\lambda+p)} - \frac{\cosh 2(\lambda-p)}{2(\lambda-p)} - \frac{\sinh 2(\lambda+p)}{4(\lambda+p)^2} + \frac{\sinh 2(\lambda-p)}{4(\lambda-p)^2}\right\} -$$

$$- \frac{q^2}{2(\lambda^2+p^2)}(\lambda \sinh 2\lambda \sin 2p - p \cosh 2\lambda \cos 2p) +$$

$$+ \frac{q^2}{4(\lambda^2+p^2)^2}\{(\lambda^2-p^2)\cosh 2\lambda \sin 2p - 2\lambda p \sinh 2\lambda \cos 2p\} -$$

$$- \frac{2q}{(2\lambda+p)^2+p^2}\{(\lambda+p)\cosh(2\lambda+p)\cos p - \lambda \sinh(2\lambda+p)\sin p\} +$$

$$+ \frac{2q}{\{(2\lambda+p)^2+p^2\}^2}\{[2(\lambda+p)^2 - p^2]\sinh(2\lambda+p)\cos p - (2\lambda^2-p^2)\cosh(2\lambda+p)\sin p\} +$$

$$+ \frac{2q}{(2\lambda-p)^2+p^2}\{(\lambda-p)\cosh(2\lambda-p)\cos p + \lambda \sinh(2\lambda-p)\sin p\} -$$

$$- \frac{2q}{\{(2\lambda-p)^2+p^2\}^2}\{[2(\lambda-p)^2 - p^2]\sinh(2\lambda-p)\cos p + (2\lambda^2-p^2)\cosh(2\lambda-p)\sin p\},$$

$$m_6 = \frac{1}{2}\left\{\frac{\sinh(\lambda+2p)}{\lambda+2p} + \frac{\sinh(\lambda-2p)}{\lambda-2p}\right\} - \frac{q^2}{\lambda^2+4p^2}(\lambda \sinh\lambda \cos 2p + 2p \cosh\lambda \sin 2p) - \alpha^2 \frac{\sinh\lambda}{\lambda},$$

$$m_7 = \frac{1}{2}\left\{\frac{\cosh(\lambda+2p)}{\lambda+2p} + \frac{\cosh(\lambda-2p)}{\lambda-2p} - \frac{\sinh(\lambda+2p)}{(\lambda+2p)^2} - \frac{\sinh(\lambda-2p)}{(\lambda-2p)^2}\right\} -$$

$$- \alpha^2\left(\frac{\cosh\lambda}{\lambda} - \frac{\sinh\lambda}{\lambda^2}\right) - \frac{q^2}{\lambda^2+4p^2}(\lambda \cosh\lambda \cos 2p + 2p \sinh\lambda \sin 2p) +$$

$$+ \frac{q^2}{(\lambda^2+4p^2)^2}\{(\lambda^2-4p^2)\sinh\lambda \cos 2p + 4\lambda p \cosh\lambda \sin 2p\},$$

$$m_8 = \frac{\sinh(\lambda+p)}{\lambda+p} + \frac{\sinh(\lambda-p)}{\lambda-p} - \frac{2q}{\lambda^2+p^2}(\lambda \sinh\lambda \cos p + p \cosh\lambda \sin p),$$

$$m_9 = \frac{\cosh(\lambda+p)}{\lambda+p} + \frac{\cosh(\lambda-p)}{\lambda-p} - \frac{\sinh(\lambda+p)}{(\lambda+p)^2} - \frac{\sinh(\lambda-p)}{(\lambda-p)^2} -$$

$$- \frac{2q}{\lambda^2+p^2}(\lambda \cosh\lambda \cos p + p \sinh\lambda \sin p) +$$

$$+ \frac{2q}{(\lambda^2+p^2)^2}\{(\lambda^2-p^2)\sinh\lambda \cos p + 2\lambda p \cosh\lambda \sin p\},$$

$$m_{10} = \frac{1}{2}\left\{\frac{\sinh(\lambda+2p)}{\lambda+2p} + \frac{\sinh(\lambda-2p)}{\lambda-2p}\right\} + \frac{q^2}{\lambda^2+4p^2}(\lambda \sinh\lambda \cos 2p + 2p \cosh\lambda \sin 2p) +$$

$$+ \beta^2 \frac{\sinh\lambda}{\lambda} - \frac{2q}{(\lambda+p)^2+p^2}\{(\lambda+p)\sinh(\lambda+p)\cos p + p \cosh(\lambda+p)\sin p\} -$$

$$- \frac{2q}{(\lambda-p)^2+p^2}\{(\lambda-p)\sinh(\lambda-p)\cos p + p \cosh(\lambda-p)\sin p\},$$

$$m_{11} = \frac{1}{2}\left\{\frac{\cosh(\lambda+2p)}{\lambda+2p} + \frac{\cosh(\lambda-2p)}{\lambda-2p} - \frac{\sinh(\lambda+2p)}{(\lambda+2p)^2} - \frac{\sinh(\lambda-2p)}{(\lambda-2p)^2}\right\} +$$

$$+ \beta^2\left(\frac{\cosh\lambda}{\lambda} - \frac{\sinh\lambda}{\lambda^2}\right) + \frac{q^2}{\lambda^2+4p^2}(\lambda\cosh\lambda\cos 2p + 2p\sinh\lambda\sin 2p) -$$

$$- \frac{q^2}{(\lambda^2+4p^2)^2}\{(\lambda^2-4p^2)\sinh\lambda\cos 2p + 4\lambda p\cosh\lambda\sin 2p\} -$$

$$- \frac{2q}{(\lambda+p)^2+p^2}\{(\lambda+p)\cosh(\lambda+p)\cos p + p\sinh(\lambda+p)\sin p\} -$$

$$- \frac{2q}{\{(\lambda+p)^2+p^2\}^2}\{[(\lambda+p)^2-p^2]\sinh(\lambda+p)\cos p + 2(\lambda+p)p\cosh(\lambda+p)\sin p\} -$$

$$- \frac{2q}{(\lambda-p)^2+p^2}\{(\lambda-p)\cosh(\lambda-p)\cos p + p\sinh(\lambda-p)\sin p\} -$$

$$- \frac{2q}{\{(\lambda-p)^2+p^2\}^2}\{[(\lambda-p)^2-p^2]\sinh(\lambda-p)\cos p + 2(\lambda-p)p\cosh(\lambda-p)\sin p\},$$

$$m_{12} = \frac{1}{2}\left\{\frac{\sinh(\lambda+2p)}{\lambda+2p} - \frac{\sinh(\lambda-2p)}{\lambda-2p}\right\} - \frac{q^2}{\lambda^2+4p^2}(\lambda\cosh\lambda\sin 2p - 2p\sinh\lambda\cos 2p) -$$

$$- \frac{q}{(\lambda+p)^2+p^2}\{(\lambda+2p)\sinh(\lambda+p)\cos p - \lambda\cosh(\lambda+p)\sin p\} +$$

$$+ \frac{q}{(\lambda-p)^2+p^2}\{(\lambda-2p)\sinh(\lambda-p)\cos p + \lambda\cosh(\lambda-p)\sin p\},$$

$$m_{13} = \frac{1}{2}\left\{\frac{\cosh(\lambda+2p)}{\lambda+2p} - \frac{\cosh(\lambda-2p)}{\lambda-2p} - \frac{\sinh(\lambda+2p)}{(\lambda+2p)^2} + \frac{\sinh(\lambda-2p)}{(\lambda-2p)^2}\right\} -$$

$$- \frac{q^2}{\lambda^2+4p^2}(\lambda\sinh\lambda\sin 2p - 2p\cosh\lambda\cos 2p) +$$

$$+ \frac{q^2}{(\lambda^2+4p^2)^2}\{(\lambda^2-2p^2)\cosh\lambda\sin 2p - 4\lambda p\sinh\lambda\cos 2p\} -$$

$$- \frac{q}{(\lambda+p)^2+p^2}\{(\lambda+2p)\cosh(\lambda+p)\cos p - \lambda\sinh(\lambda+p)\sin p\} +$$

$$+ \frac{q}{\{(\lambda+p)^2+p^2\}^2}\{[(\lambda+2p)^2-2p^2]\sinh(\lambda+p)\cos p - (\lambda^2-2p^2)\cosh(\lambda+p)\sin p\} +$$

$$+ \frac{q}{(\lambda-p)^2+p^2}\{(\lambda-2p)\cosh(\lambda-p)\cos p + \lambda\sinh(\lambda-p)\sin p\} -$$

$$- \frac{q}{\{(\lambda-p)^2+p^2\}^2}\{[(\lambda-2p)^2-2p^2]\sinh(\lambda-p)\cos p + (\lambda^2-2p^2)\cosh(\lambda-p)\sin p\}.$$

2. *Panel with Simply-Supported Edges.*

$$n_0 = -\frac{\pi^2}{4\lambda^2+\pi^2}\frac{\sinh 2\lambda}{2\lambda},$$

$$n_1 = -\frac{\pi^2}{4\lambda^2+\pi^2}\frac{\cosh 2\lambda}{2\lambda} + \frac{\pi^2(12\lambda^2+\pi^2)}{(4\lambda^2+\pi^2)^2}\frac{\sinh 2\lambda}{4\lambda^2},$$

$$n_2 = -\frac{\pi}{4\lambda^2+\pi^2}\sinh 2\lambda,$$

$$n_3 = -\frac{\pi}{4\lambda^2+\pi^2}\cosh 2\lambda + \frac{4\lambda\pi}{(4\lambda^2+\pi^2)^2}\sinh 2\lambda,$$

$$n_4 = -\frac{\pi^2}{\lambda^2+\pi^2}\frac{\sinh \lambda}{\lambda},$$

$$n_5 = -\frac{\pi^2}{\lambda^2+\pi^2}\frac{\cosh \lambda}{\lambda} + \frac{\pi^2(3\lambda^2+\pi^2)}{(\lambda^2+\pi^2)^2}\frac{\sinh \lambda}{\lambda^2},$$

$$n_6 = \frac{4\pi}{4\lambda^2+\pi^2}\cosh \lambda,$$

$$n_7 = \frac{4\pi}{4\lambda^2+\pi^2}\sinh \lambda - \frac{32\lambda\pi}{(4\lambda^2+\pi^2)^2}\cosh \lambda,$$

$$n_8 = -\frac{\pi}{\lambda^2+\pi^2}\sinh \lambda,$$

$$n_9 = -\frac{\pi}{\lambda^2+\pi^2}\cosh \lambda + \frac{2\lambda\pi}{(\lambda^2+\pi^2)^2}\sinh \lambda.$$

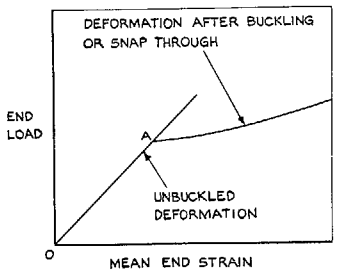

(a) GENERAL FORM OF THEORETICAL RESULTS

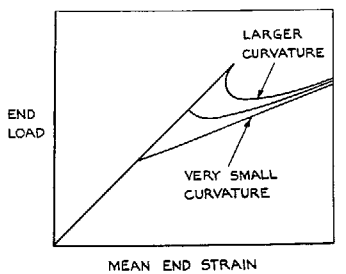

(b) INFLUENCE OF CURVATURE ON BUCKLING OF PANEL WITH SIDES FREE TO MOVE CIRCUMFERENTIALLY.

FIGS. 1a and b. General form of load/(end strain) curves.

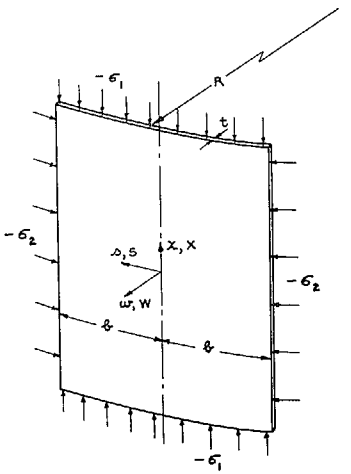

FIG. 2. Notation.

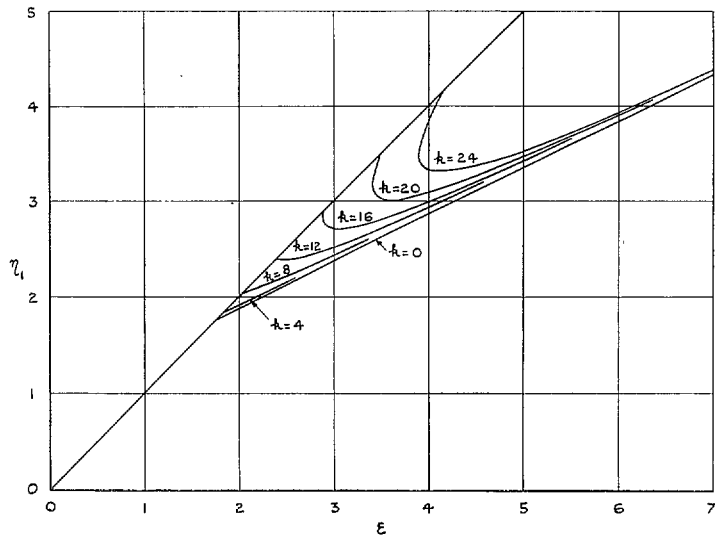

FIG. 3. Load/(end strain) curves for clamped panels with sides unrestrained in the middle surface.

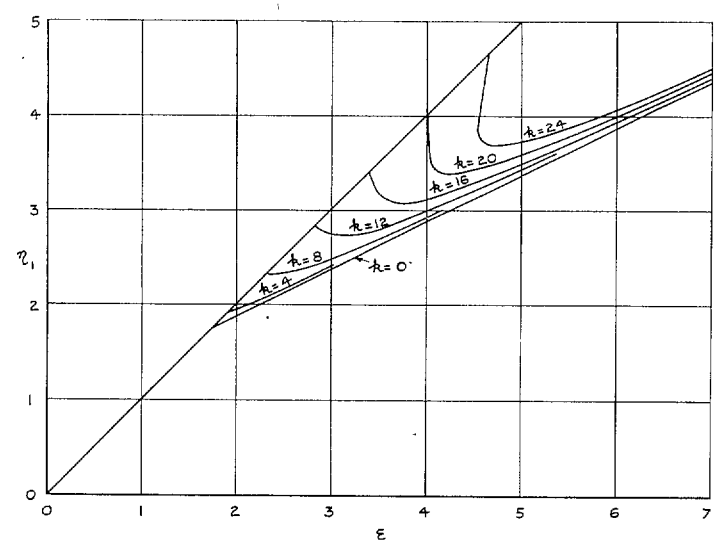

FIG. 4. Load/(end strain) curves for clamped panels with sides held straight but free to move circumferentially.

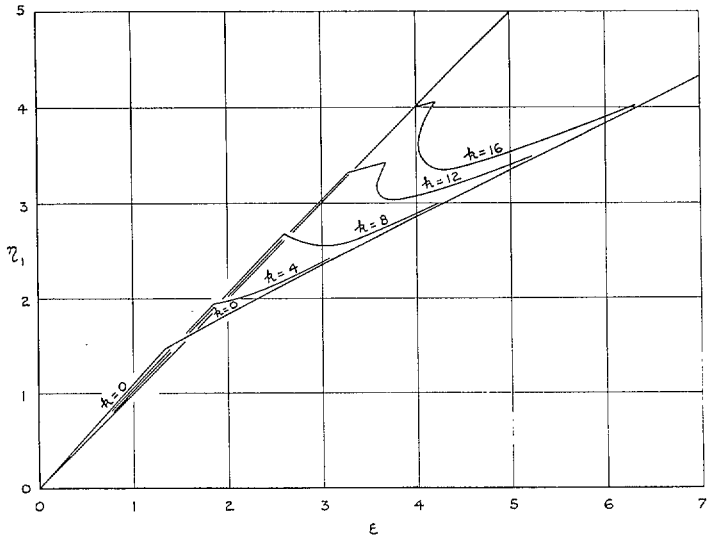

FIG. 5. Load/(end strain) curves for clamped panels with sides held straight and prevented from moving circumferentially.

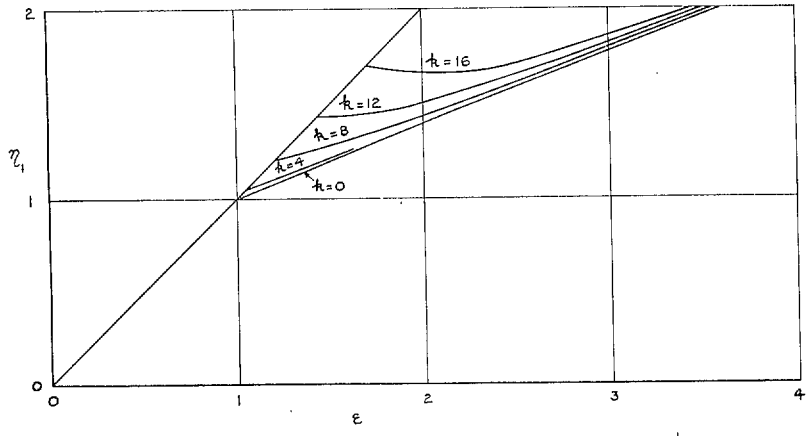

FIG. 6. Load/(end strain) curves for simply-supported panels with sides unrestrained in the middle surface.

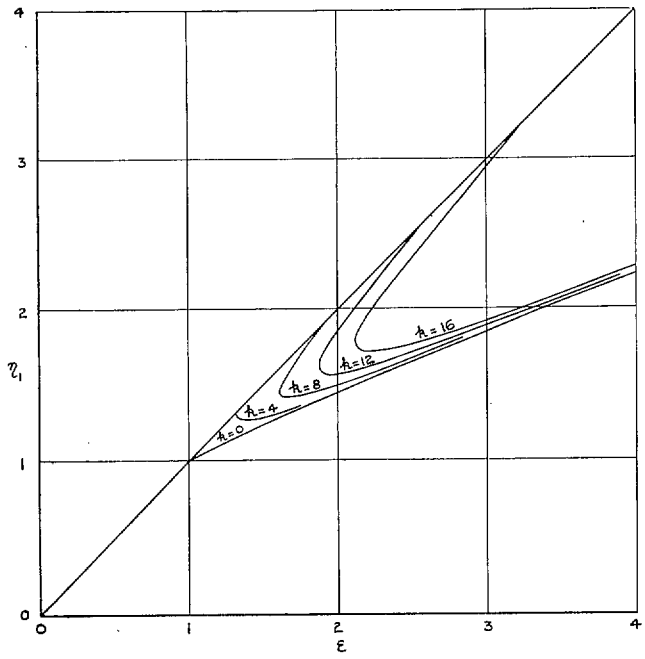

FIG. 7. Load/(end strain) curves for simply-supported panels with sides held straight but free to move circumferentially.

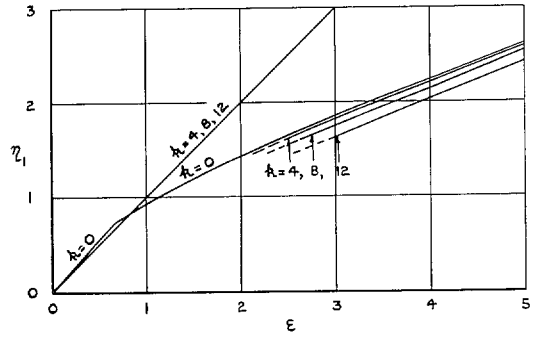

FIG. 8. Load/(end strain) curves for simply-supported panels with sides held straight and prevented from moving circumferentially.

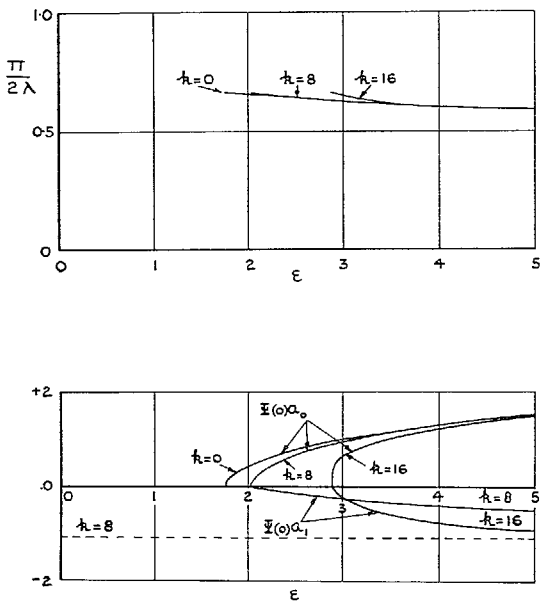

THE DASHED LINE DENOTES THE VALUE OF $\Xi(o)a_1$ NECESSARY FOR THE MEAN DEFLECTION OF THE CENTRE-LINE TO LIE IN THE PLANE CONTAINING THE SIDES.

FIG. 9. Waveform parameters. Clamped panels with sides unrestrained in the middle surface.

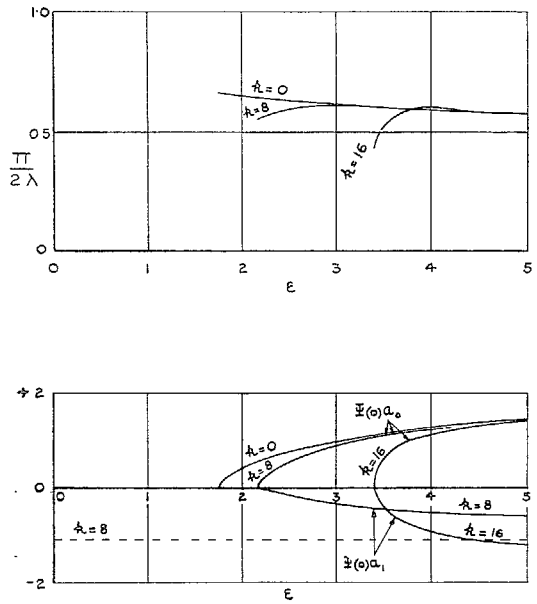

THE DASHED LINE IS DEFINED IN FIG. 9.

FIG. 10. Waveform parameters. Clamped panels with sides held straight but free to move circumferentially.

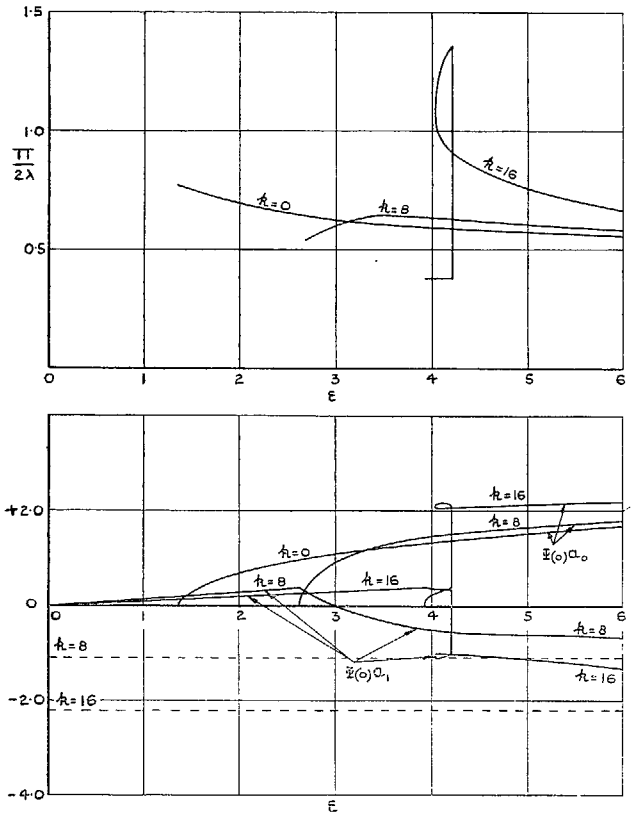

FIG. 11. Waveform parameters. Clamped panels with sides held straight and prevented from moving circumferentially.

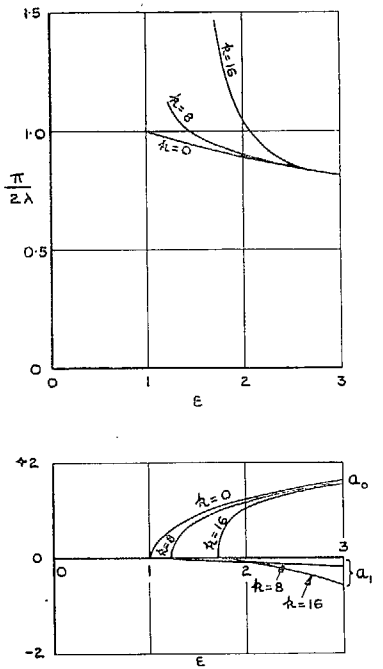

FIG. 12. Waveform parameters. Simply-supported panels with sides unrestrained in the middle surface.

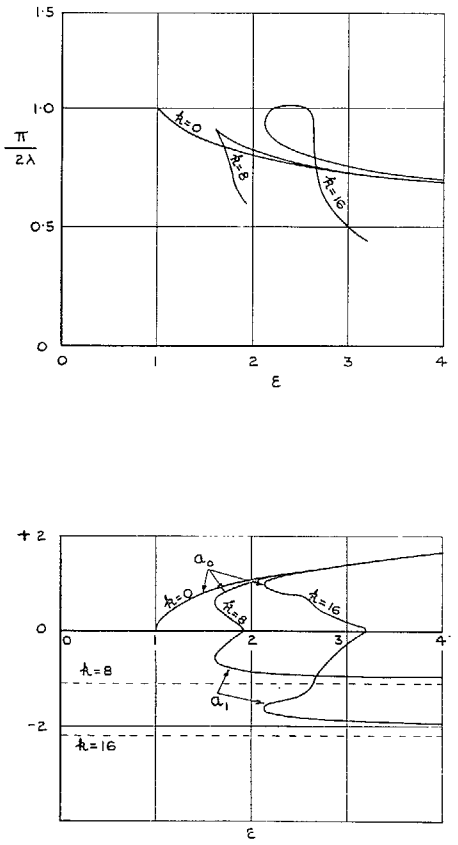

FIG. 13. Waveform parameters. Simply-supported panels with sides held straight but free to move circumferentially.

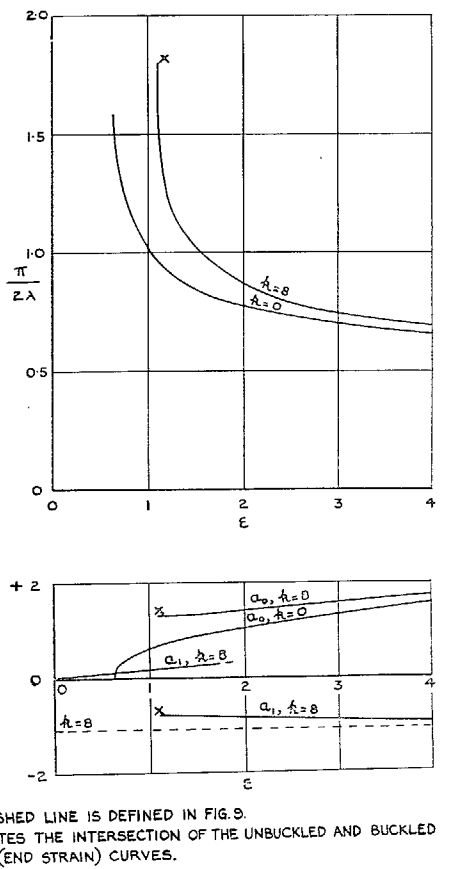

FIG. 14. Waveform parameters. Simply-supported panels with sides held straight and prevented from moving circumferentially.

(90631) Wt. 66/2301 K.5 1/65 Hw.

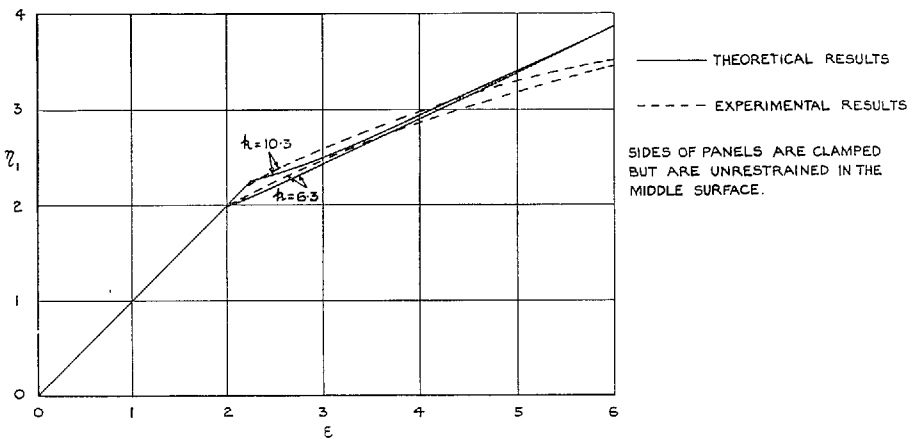

FIG. 15. Comparison of theoretical and experimental load/(end strain) curves.

Publications of the Aeronautical Research Council

ANNUAL TECHNICAL REPORTS OF THE AERONAUTICAL RESEARCH COUNCIL (BOUND VOLUMES)

1942 Vol. I. Aero and Hydrodynamics, Aerofoils, Airscrews, Engines. 75*s.* (post 2*s.* 9*d.*)
Vol. II. Noise, Parachutes, Stability and Control, Structures, Vibration, Wind Tunnels. 47*s.* 6*d.* (post 2*s.* 3*d.*)

1943 Vol. I. Aerodynamics, Aerofoils, Airscrews. 80*s.* (post 2*s.* 6*d.*)
Vol. II. Engines, Flutter, Materials, Parachutes, Performance, Stability and Control, Structures. 90*s.* (post 2*s.* 9*d.*)

1944 Vol. I. Aero and Hydrodynamics, Aerofoils, Aircraft, Airscrews, Controls. 84*s.* (post 3*s.*)
Vol. II. Flutter and Vibration, Materials, Miscellaneous, Navigation, Parachutes, Performance, Plates and Panels, Stability, Structures, Test Equipment, Wind Tunnels. 84*s.* (post 3*s.*)

1945 Vol. I. Aero and Hydrodynamics, Aerofoils. 130*s.* (post 3*s.* 6*d.*)
Vol. II. Aircraft, Airscrews, Controls. 130*s.* (post 3*s.* 6*d.*)
Vol. III. Flutter and Vibration, Instruments, Miscellaneous, Parachutes, Plates and Panels, Propulsion. 130*s.* (post 3*s.* 3*d.*)
Vol. IV. Stability, Structures, Wind Tunnels, Wind Tunnel Technique. 130*s.* (post 3*s.* 3*d.*)

1946 Vol. I. Accidents, Aerodynamics, Aerofoils and Hydrofoils. 168*s.* (post 3*s.* 9*d.*)
Vol. II. Airscrews, Cabin Cooling, Chemical Hazards, Controls, Flames, Flutter, Helicopters, Instruments and Instrumentation, Interference, Jets, Miscellaneous, Parachutes. 168*s.* (post 3*s.* 3*d.*)
Vol. III. Performance, Propulsion, Seaplanes, Stability, Structures, Wind Tunnels. 168*s.* (post 3*s.* 6*d.*)

1947 Vol. I. Aerodynamics, Aerofoils, Aircraft. 168*s.* (post 3*s.* 9*d.*)
Vol. II. Airscrews and Rotors, Controls, Flutter, Materials, Miscellaneous, Parachutes, Propulsion, Seaplanes, Stability, Structures, Take-off and Landing. 168*s.* (post 3*s.* 9*d.*)

1948 Vol. I. Aerodynamics, Aerofoils, Aircraft, Airscrews, Controls, Flutter and Vibration, Helicopters, Instruments, Propulsion, Seaplane, Stability, Structures, Wind Tunnels. 130*s.* (post 3*s.* 3*d.*)
Vol. II. Aerodynamics, Aerofoils, Aircraft, Airscrews, Controls, Flutter and Vibration, Helicopters, Instruments, Propulsion, Seaplane, Stability, Structures, Wind Tunnels. 110*s.* (post 3*s.* 3*d.*)

Special Volumes

Vol. I. Aero and Hydrodynamics, Aerofoils, Controls, Flutter, Kites, Parachutes, Performance, Propulsion, Stability. 126*s.* (post 3*s.*)
Vol. II. Aero and Hydrodynamics, Aerofoils, Airscrews, Controls, Flutter, Materials, Miscellaneous, Parachutes, Propulsion, Stability, Structures. 147*s.* (post 3*s.*)
Vol. III. Aero and Hydrodynamics, Aerofoils, Airscrews, Controls, Flutter, Kites, Miscellaneous, Parachutes, Propulsion, Seaplanes, Stability, Structures, Test Equipment. 189*s.* (post 3*s.* 9*d.*)

Reviews of the Aeronautical Research Council

1939–48 3*s.* (post 6*d.*) 1949–54 5*s.* (post 5*d.*)

Index to all Reports and Memoranda published in the Annual Technical Reports

1909–1947 R. & M. 2600 (out of print)

Indexes to the Reports and Memoranda of the Aeronautical Research Council

Between Nos. 2351–2449	R. & M. No. 2450 2*s.* (post 3*d.*)
Between Nos. 2451–2549	R. & M. No. 2550 2*s.* 6*d.* (post 3*d.*)
Between Nos. 2551–2649	R. & M. No. 2650 2*s.* 6*d.* (post 3*d.*)
Between Nos. 2651–2749	R. & M. No. 2750 2*s.* 6*d.* (post 3*d.*)
Between Nos. 2751–2849	R. & M. No. 2850 2*s.* 6*d.* (post 3*d.*)
Between Nos. 2851–2949	R. & M. No. 2950 3*s.* (post 3*d.*)
Between Nos. 2951–3049	R. & M. No. 3050 3*s.* 6*d.* (post 3*d.*)
Between Nos. 3051–3149	R. & M. No. 3150 3*s.* 6*d.* (post 3*d.*)

HER MAJESTY'S STATIONERY OFFICE

from the addresses overleaf

Printed and published by
HER MAJESTY'S STATIONERY OFFICE

To be purchased from
York House, Kingsway, London w.c.2
423 Oxford Street, London w.1
13A Castle Street, Edinburgh 2
109 St. Mary Street, Cardiff
39 King Street, Manchester 2
50 Fairfax Street, Bristol 1
35 Smallbrook, Ringway, Birmingham 5
80 Chichester Street, Belfast 1
or through any bookseller

Printed in England

S.O. Code No. 23-3392